May 13, 2010

Light-induced Self-synchronizing Flow Patterns

Elad Greenfield
Carmel Rotschild
Alexander Szameit
Jonathan Nemirovsky
Ramy El-Ganainy, *University of Central Florida*, et al.

Light-induced self-synchronizing flow patterns

2011 New J. Phys. 13 053021

(http://iopscience.iop.org/1367-2630/13/5/053021)

New Journal of Physics
The open-access journal for physics

Light-induced self-synchronizing flow patterns

Elad Greenfield[1], Carmel Rotschild[1], Alexander Szameit[1], Jonathan Nemirovsky[1], Ramy El-Ganainy[2], Demetrios N Christodoulides[2], Meirav Saraf[3], Efrat Lifshitz[3] and Mordechai Segev[1,4]

[1] Physics Department and Solid State Institute, Technion, Haifa 32000, Israel
[2] CREOL—College of Optics and Photonics, University of Central Florida, Orlando, FL 32816, USA
[3] Chemistry Department and Solid State Institute, Technion, Haifa 32000, Israel
E-mail: msegev@tx.technion.ac.il

New Journal of Physics **13** (2011) 053021 (12pp)
Received 22 December 2010
Published 13 May 2011
Online at http://www.njp.org/
doi:10.1088/1367-2630/13/5/053021

Abstract. In this paper, we present the observation of light-induced self-synchronizing flow patterns in a light–fluid system. A light beam induces local flow patterns in a fluid, which oscillate periodically or chaotically in time. The oscillations within different regions of the fluid interact with each other through heat- and surface-tension-induced fluid waves, and they become synchronized. We demonstrate optical control over the state of synchronization and over the temporal correlation between different parts of the flow field. Finally, we provide a model to elucidate these results and we suggest further ideas on light controlling flow and vice versa.

S Online supplementary data available from stacks.iop.org/NJP/13/053021/mmedia

[4] Author to whom any correspondence should be addressed.

Contents

1. Introduction

Light–fluid interactions give rise to phenomena that are fundamentally different from those encountered in light–solid interactions. The mobility of the fluid, the possibility of optically inducing deformations in the flow field, the profound role of diffusion and convection in transporting heat and substance and the large-scale heterogeneities emerging when a fluid interacts with light—all these contribute to a variety of nonlinear phenomena that are not usually encountered in the case when light interacts with solids. Examples of such phenomena range from optically induced flow [1]–[6] and light-induced instabilities and chaotic dynamics of flow mechanics [7]–[10], to nonlinear optical effects such as the self-focusing and self-channeling of light in colloidal suspensions [11]–[14]. However, the nonlinear dynamics of light and fluid, far from steady state, is currently understudied. Such nonlinear dynamics often offers a variety of interesting complex phenomena and functionality, which has not yet been demonstrated in a coupled light–fluid system.

Here, we report the experimental observation of self-synchronizing light-induced flow patterns in a light–fluid system exhibiting far from steady-state dynamics. In this system, the light induces heat-driven local flow patterns in different regions of the fluid. These flow patterns self-oscillate with time, either periodically or chaotically. The local light–fluid oscillations in different regions in the fluid interact with one another through light and fluid waves, and these oscillations synchronize. Nontrivially, this highly complex nonlinear system can be controlled externally: adjusting the (external) experimental conditions, such as the laser power and the beam position in the fluid, we demonstrate optical control over the state of synchronization between the local flow patterns. That is, we control the temporal correlation between different parts of the flow field by adjusting these two 'knobs'. Specifically, we demonstrate experimentally transitions between various light-induced states of synchronized flow patterns: periodic flow patterns that are synchronized in-phase with one another, periodic patterns that are unsynchronized and disturb each other irregularly, a periodic flow pattern that becomes synchronized to a chaotic flow pattern while remaining periodic, and a chaotic flow pattern that drives a periodic flow pattern to chaos. We gain insights into the origin of the synchronization phenomena by showing that the system comprises a set of heat-accumulating, 'leaky', light–fluid relaxation oscillators [15]–[17], where the leakage of heat from one oscillator excites another oscillator. We present an asymmetric 'integrate and fire'-type model that elucidates these results.

2. Experimental apparatus

Our experimental system resembles the light–fluid system studied in the 1980s by Gouesbet *et al* [7]–[10], who, in a series of pioneering experiments, demonstrated thermal lens oscillations. The system consists of a laser beam propagating in a liquid suspension of nanometer-sized colloids, designed to absorb light. The system, contained in a glass cell, is depicted in figure 1, along with the accompanying measurement apparatus. The continuous-wave laser beam enters the cell from the right. We tightly focus the beam roughly 1 mm below the liquid–air interface, and examine the dynamics of both the light and the fluid, in real time. When the laser power is increased above a certain level, the fluid–air surface interfacial meniscus and the laser beam itself start to oscillate together. The oscillations are manifested in large, coupled, periodic motions of both the trajectory of the beam and of the surface meniscus. Figure 1(a) presents the visual effect at two extremes of an oscillation cycle: the beam trajectory moves up and down in a perfectly periodic manner, oscillating between the two states presented in the figure. Movie 1 in the supplementary material (available from stacks.iop.org/NJP/13/053021/mmedia) displays the visible oscillations of the laser beam trajectory.

We investigate the light–fluid oscillation in real time using two independent apparatuses, as sketched in figure 1(b). The trajectory of the optical beam is recorded by a quad-photodiode detector, mapping the vertical and horizontal positions of the beam at the output facet of the liquid cell (figure 1(b) displays a typical signal). In addition, we constructed a fast phase-imaging ('Schlieren' and shadowgraph) system that converts the phase of a collimated white-light beam traversing the cell perpendicular to the laser beam path (see figure 1(b)) into intensity contrast images. The broad white-light beam ('plane wave') entering the liquid cell acquires nonplanar phase, determined by the (laser-induced) refractive index distribution in the cell. A knife edge filter at the Fourier plane of a lens (placed a focal distance away from the output plane of the cell) converts this phase structure into an intensity structure, which can be recorded with another (subsequent) lens and a digital camera.

The 'Schlieren' system thus provides real-time information about the laser–liquid interaction dynamics. Figure 1(c) is a typical phase-image displaying the refractive index distribution forming in the cell. Darker regions indicate a lower refractive index, corresponding to regions of higher temperature. For instance, in figure 1(c) the completely dark region corresponds to a temperature difference of $\sim 30\,^{\circ}\mathrm{C}$ from the ambient (room) temperature, and the refractive index changes observed are of the order of $\delta n \sim 10^{-2}$. The way these quantities are obtained and a discussion on the mechanisms responsible for the refractive index and temperature changes are described in section B of the supplementary material (PDF). Notably, the light–fluid interaction bends the beam trajectory downwards, as clearly seen by the naked eye and as monitored using the quad detector (figure 1(b)). The explanation of the beam bending effect is as follows. The light is absorbed in the fluid, which heats the liquid mostly at the beam waist. Warmer fluid is less dense and consequently rises upward towards the surface meniscus. In this liquid, the refractive index decreases as the temperature increases; hence the warmer fluid above the beam has a lower refractive index than the fluid below the beam. Since light is always 'attracted' towards higher refractive index, the beam bends downwards.

The detector and the side-viewing Schlieren system simultaneously provide information about the changes in trajectory of the optical beam and the real-time refractive-index redistribution causing this change. In the supplementary material, we present technical details of the Schlieren system as well as a typical Schlieren movie showing the dynamics inside the liquid (movie 2).

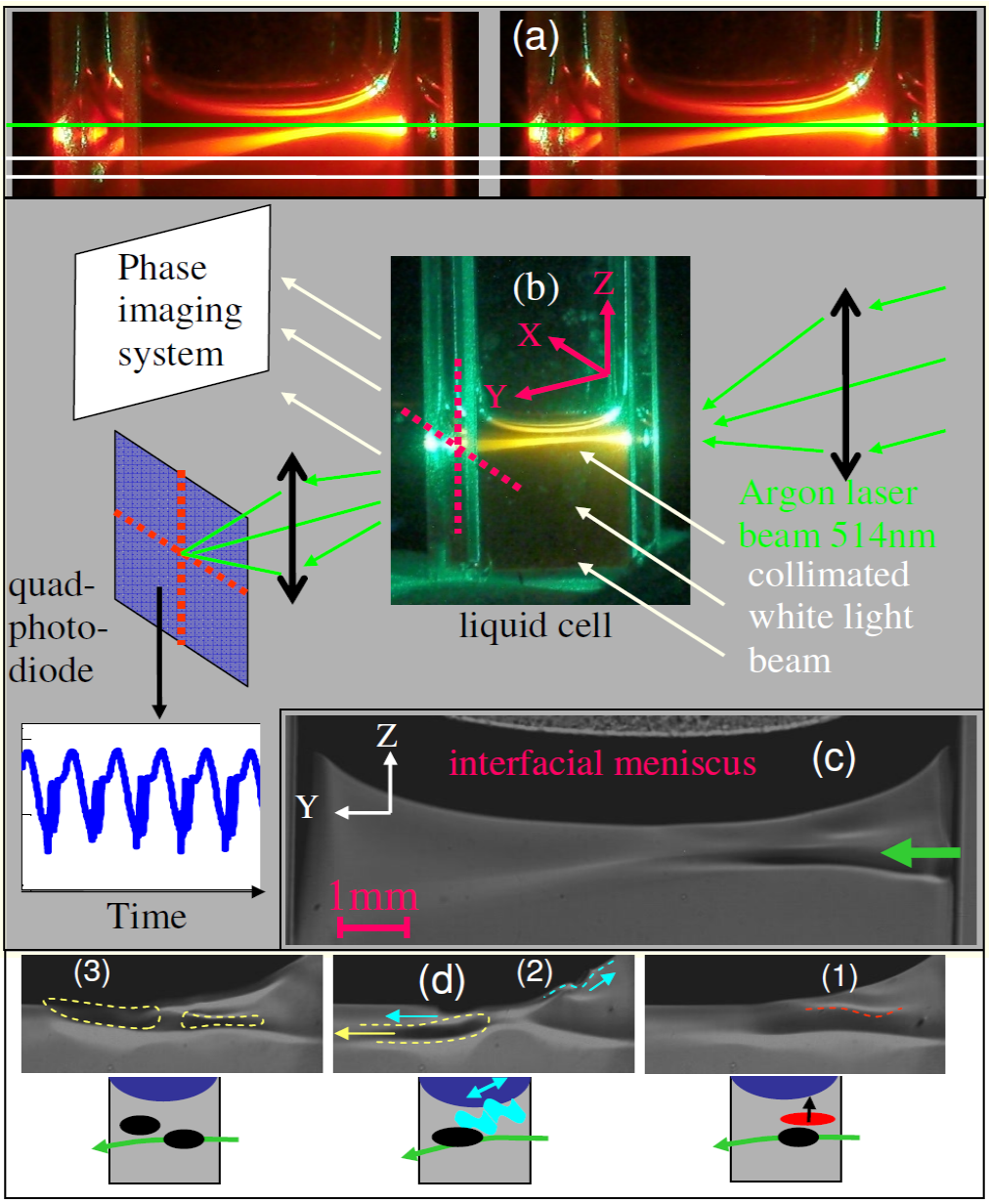

Figure 1. The phenomenon of light–fluid oscillations and the experimental setup designed to monitor the dynamics of the heat waves in the fluid and light separately. (a) Photographs of the two extreme states of a typical oscillation cycle. The beam enters on the right, with its center marked by the green markers. In the oscillatory regime, the beam alternates between two states of shallower (right image) and steeper (left image) angles. The white markers identify the difference in the trajectories of the beams exiting the cell. (b) Schematics of the experimental system and the apparatuses designed to monitor the dynamics of the light and fluid (not to scale). (c) Typical phase image (laser beam marked with a green arrow). (d) The mechanism underlying the oscillatory dynamics. At each oscillation, light-induced liquid flow and heat waves modify the refractive index distribution in the beam path, resulting in periodic deflection of the light-beam trajectory.

Figure 1(d) shows the sequence of processes governing a typical light–fluid oscillation. In each oscillation, heat accumulates in the fluid, and a layer of hot fluid (red dashed line in panel (1) and red ellipse in the illustration) detaches from the beam waist and rises towards the surface meniscus. When the rising layer reaches the surface, it triggers surface-tension instability, resulting in a 'hydrothermal wave' [9]. Such waves couple surface deflections to the shear flow of the fluid underlying the surface meniscus [9] (cyan dashed line in panel (2) and cyan waveforms in the illustration), and their propagation is both along the surface and in the bulk. These waves drive the hot fluid from the surface back into the beam waist in the bulk. The hot liquid (marked in yellow in panel (2)) driven back into the beam waist is accompanied by a change in the refractive index of the fluid, directly affecting the trajectory of the laser beam inside the fluid. We identify these light–fluid oscillations as a 'self-sustained oscillator' [17], a nonlinear oscillator whose frequencies and amplitudes of oscillation are set by its internal feedback dynamics, as opposed to external forcing at a predetermined frequency.

3. Observation of light-induced self-synchronizing flow patterns

The light–fluid oscillations reported in section 2 have been reported previously [7]–[10]. In the supplementary material we present some aspects of the transition to chaos of such light–fluid oscillations, which were not reported before. Here, however, our main focus is on new dynamic phenomena arising from the interactions between light–fluid oscillations at different locations in the fluid.

For certain system parameters, the hydrothermal surface waves and bulk waves generated by the light–fluid self-sustained oscillator suffice to make the hot fluid rise upward at an adjacent region in the fluid, which is already unstable due to heating by the laser beam. Hence, in the same setting of figure 1(d), the light–fluid self-sustained oscillator induces another (at least one) self-sustained oscillator. Each self-sustained oscillator creates a particular flow pattern in the region of the fluid where it acts, where the flow can be either periodic at a predetermined frequency or chaotic. The oscillators couple to one another through the dynamics of the light, heat and fluid, and the flow patterns of different regions synchronize in phase as they evolve with time.

Figure 2 shows how two light–fluid oscillators couple and influence each other's phase of oscillations. At time $t = 0$, two distinct layers of hot fluid rise to the surface (on the left and on the right of the green marker), defining the regions where the two oscillators act (henceforth referred to as the right oscillator and the left oscillator, respectively). The rising fluid layer belonging to the right oscillator reaches the surface before the layer belonging to the left oscillator does. It excites a surface-tension instability there (shown at $t = 160$ ms and marked with an orange dashed line and 'X' mark), sending a hot-fluid wave (shown at $t = 195$ ms, and marked by yellow dashed lines and arrows) into the left oscillator's region. The hot fluid that is driven into the left oscillator (marked with white dashed lines on the $t = 300$ ms image) consequently triggers a response: surface instability forms (shown at $t = 355$ ms, marked with an orange dashed line and 'X' mark) in the left oscillator's region, sending a hot-fluid wave into the right oscillator (the wave is shown at $t = 415$ ms, and marked with yellow dashed lines and arrows). This wave in turn affects the dynamics of the right oscillator—and ends one complete cycle of mutually coupled oscillations. The complex, dynamically varying shape of the heat profile (which corresponds to the refractive index profile) is clearly visible in figure 2.

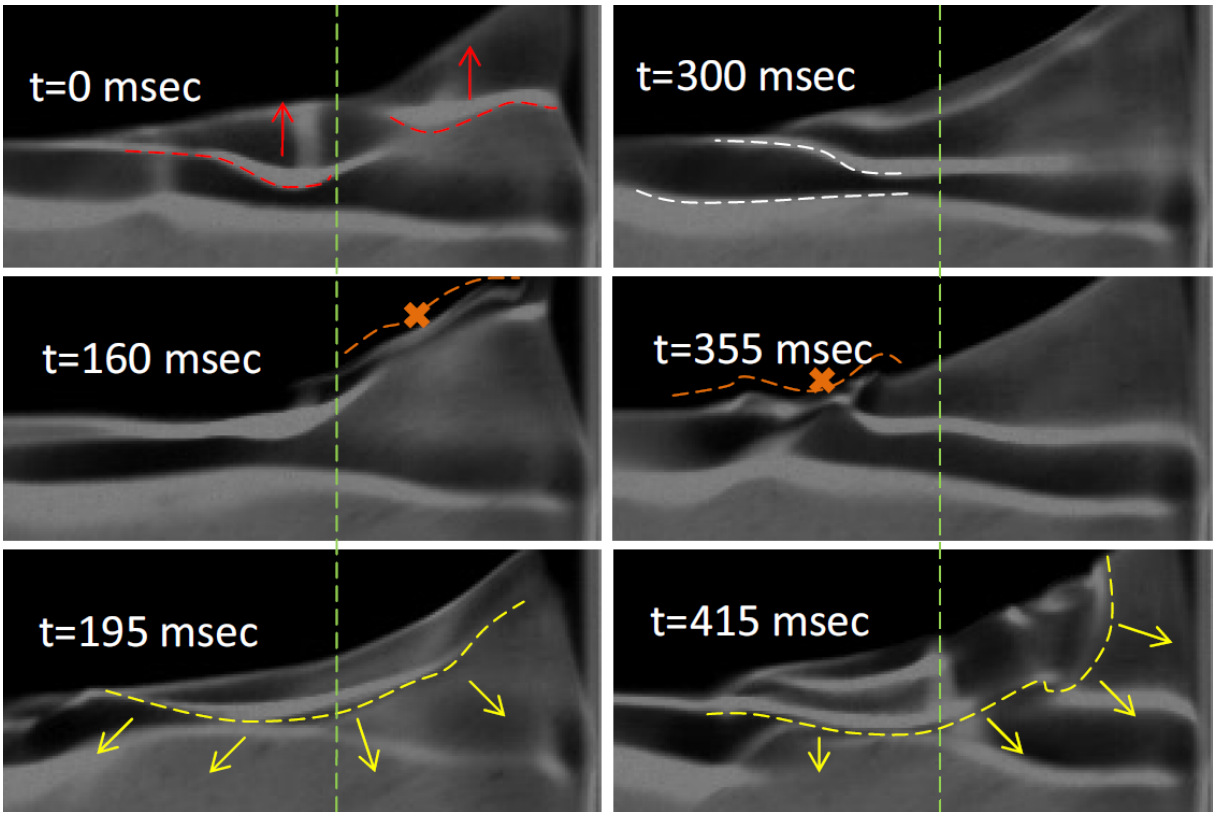

Figure 2. Schlieren images showing one cycle of mutual coupling between two adjacent light–fluid oscillators. The oscillators couple and perturb each other's phases through the hydrothermal waves that they emanate, and their sharing of the same light beam as the heat source.

The interaction between the light–fluid oscillators leads to several regimes of mutual phase synchronization and frequency entrainment, which are all accessible by properly adjusting our 'knobs': the laser beam power and input beam distance from the interfacial meniscus. By externally varying these external parameters, we modify and control each light–fluid oscillator (such as those in figure 2) individually, as well as their interaction with one another. Consequently, we control the extent of synchronization between the light–fluid oscillators on the right and left parts of images, such as those in figure 2, where 'synchronization of the oscillators' means the temporal correlation between their corresponding fluid-flow fields.

Figure 3 presents the results of such an experiment, in which the input laser beam is moved towards the surface meniscus in five steps (corresponding to figures 3(i)–(v)). Due to the geometry of the meniscus, as the input laser beam is moved vertically upward, its relative distance to the surface changes only slightly in the region on the right of the cell (right part of the images in figure 2), whereas it changes appreciably more in the left part of the cell. Consequently, as the beam moves closer to the surface, the light–fluid oscillator on the left experiences a significant change in its oscillation frequency, periodic or chaotic nature, its amplitude of oscillation and the strength of the surface waves it emanates, but the light–fluid oscillator on the right remains periodic, and its dynamics changes only a little throughout the

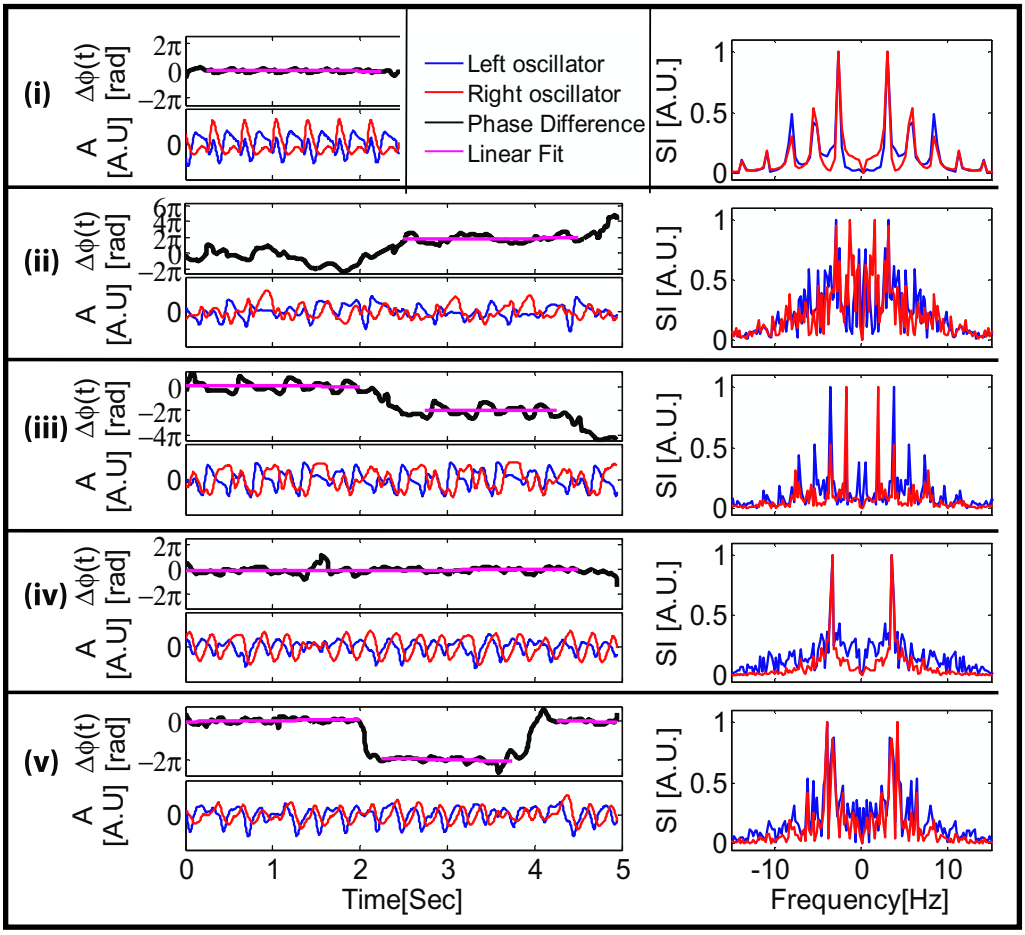

Figure 3. Externally modifying the synchronization and temporal correlation between two light-induced flow patterns located at different parts of a fluid. The laser beam was moved vertically in the fluid towards the surface meniscus in five steps (corresponding to panels (i)–(v)). With each step and the accompanying change to the left oscillator, the coupling between the left and right flow fields became stronger, and their extent of synchronization changed. Panels (i)–(v) thus correspond to five distinct states of synchronization and temporal correlation between the left and right flow patterns. (i) Synchronization between two periodic light–fluid oscillators. (ii) Loss of synchronization and coupling-induced enhancement of irregular dynamics. (iii) Anti-phase synchronization of two periodic oscillators. (iv) Synchronization between one chaotic and one periodic oscillator. (v) Synchronization between two chaotic oscillators. Panels (iii) and (v) also exhibit phase slips in which synchronization is first lost and then quickly regained. The data shown here comprise a mechanism through which one can externally modify the presence of periodic and chaotic flow fields in different parts of a fluid, and control the temporal correlation between them. The dynamics described above are also visible in the movies (movies 3–7 in the supplementary material).

experiment. As the dynamics of the left oscillator changes with decreasing distance between the laser beam and the surface, the coupling between the oscillators becomes stronger, and they synchronize to a different extent.

In figures 3(i)–(v) we observe five distinct states of synchronization between the oscillators, and equivalently temporal correlation between the left and right flow patterns: (i) synchronization between two periodic flow patterns, where the right pattern synchronizes the left one; (ii) coupling-induced loss of synchronization and disruption of the periodicity of the flow patterns' oscillations; (iii) synchronization in anti-phase between two periodic flow patterns, where the joint frequency of oscillation is neither of the patterns' oscillation frequencies; (iv) synchronization between a chaotic flow pattern and a periodic flow pattern; and (v) a chaotic flow pattern synchronizing and inducing chaos in an otherwise periodic flow pattern. Since the transition between these states of synchronization is due only to a change in the position of the input beam, it comprises a mechanism by which one may externally control the presence of periodic and chaotic flow patterns in a fluid, and the temporal correlation between them.

In each panel of figure 3, the bottom left stripe shows the time evolution of the geometrical locations of the centers of heat for the right (red) and left (blue) light–fluid oscillators. These data are obtained directly from sequences of Schlieren images of the dynamics. The upper left stripe shows the phase difference $\Delta\Phi(t)$ between these signals, as obtained from their analytic expansions [17], whereas the right stripe shows their spectral intensity (power spectrum), denoted '*SI*' in the figures, corresponding to the right and left temporal oscillations (although the spectral intensities of these real signals are symmetric with respect to the zero frequency, both the negative and positive frequencies are shown). The purple lines in the phase-difference plots are linear fits to $\Delta\Phi(t)$, at time intervals at which it exhibits a plateau. During those time intervals, the constant phase difference between the oscillators indicates that the oscillations of the two oscillators are synchronized, and their frequencies entrained [17].

In what follows, we provide a detailed description of the synchronization dynamics at each panel, each manifesting a different synchronization phenomenon. The experiment commences from the initial state corresponding to the graphs in figure 3(i). The hot-fluid layer belonging to the right oscillator rises faster than the left oscillator's layer, and the surface instability always forms at the right region first. The wave that has formed sends hot fluid into the left oscillator, exciting the surface instability there, and setting the left oscillator's phase to zero. The right oscillator dominates the phase of the left oscillator, and the oscillators are synchronized, as is apparent from their $\Delta\Phi = 0$ plateau. This behavior is apparent in movie 3 in the supplementary material.

In figure 3(ii), the input laser beam has been moved one step closer to the surface meniscus. The left oscillator's hot-fluid layer rises more quickly. Sometimes the left oscillator excites a surface instability before the right oscillator, and sometimes it is the other way around. Whereas each oscillator seems to individually tend to periodic dynamics, their coupled action disturbs each other's dynamics in an irregular fashion; hence their joint dynamics is nonperiodic. This is clearly indicated by the continuous power spectra of the oscillators, and in movie 4 of the supplementary material. The oscillators are generally not synchronized, as is apparent from their phase difference ranging between -2π and 4π with time, although a short plateau does appear in $\Delta\Phi = -2\pi$.

In figure 3(iii), the laser beam was moved a second step closer to the surface meniscus. The surface wave emanating from the right oscillator is sufficient to trigger surface instability in the left oscillator, resetting its phase to zero. The left oscillator emanates a surface wave in return,

which meets the rising layer of fluid of the right oscillator, delaying its phase but not exciting its surface instability. The result is anti-phase periodic synchronization between the oscillators, as visible to the naked eye in movie 5 of the supplementary material. Note that the spectrum in figure 3(iii) regains periodic dynamics: it is the self-synchronization between the oscillators that results in periodic modification of one another's phase, suppressing the chaos observed in figure 3(ii). The phase difference data in figure 3(iii) also exhibits $\pm 2\pi$ sharp 'stairs'. These stairs are phase slips, in which synchronization is temporarily lost and is subsequently quickly regained.

In figures 3(iv) and (v), the laser beam was moved a third and a fourth step closer to the surface meniscus. The left oscillator becomes chaotic by itself, and it dominates the phase dynamics of the system. In figure 3(iv), the left oscillator emanates an irregular sequence of surface waves, but only those that are at its dominant frequency are strong enough to propagate and influence the right oscillator, as is apparent in movie 6 of the supplementary material. Hence, the right oscillator's phase is controlled only by the dominant spectral component of a chaotic left oscillator. The right oscillator remains periodic, while the left oscillator is chaotic, yet they are still synchronized with $\Delta\Phi = 0$. In figure 3(v), more spectral components of the left oscillator's surface waves become strong enough to influence the phase of the right oscillator, and the right oscillator also becomes chaotic. The oscillators retain synchronization, displaying 'stair-like' phase slips. This situation is visible in movie 7 of the supplementary material.

4. Theoretical model and discussion

We offer an interpretation of the synchronization phenomena in the framework of nonlinear dynamic systems. The interpretation is based on experimental proof, which we present in detail in the supplementary material. Here, we stop with the summary of these results and conclusions. We identify each light–fluid oscillator as a self-sustained oscillator, and more specifically, a relaxation oscillator [15]–[17], an oscillator that slowly accumulates some quantity (in our case heat) and then quickly runs out of this quantity once it reaches a certain level. We detect a 'memory' that the relaxation oscillator realizes, which dictates its transition to chaos. The memory is comprised of hot fluid that resides in a reservoir after each oscillation, affecting the dynamics of the oscillation that follows. This memory is directly measurable with the Schlieren phase imaging apparatus, and it underlies the period-doubling bifurcation route leading a single light–fluid oscillator to chaos (measurements of this route to chaos and characterization of chaotic states can be found in section D of the supplementary material). This type of memory in chaotic relaxation oscillators had been reported in natural and man-made systems [15]. But our system has another characteristic: the oscillator 'leaks' the quantity it accumulates—heat, to adjacent locations in the fluid. A light–fluid oscillator is created whenever there is a strong enough local temperature gradient at some location in the fluid—and the heat leaking from one oscillator may provide a strong enough gradient near its location. Hence, the leakage of heat from one oscillator drives other oscillators at adjacent locations in the fluid into motion. Since the new oscillator would not exist if it were not for this 'leakage of heat', the oscillators are *a priori* asymmetrically coupled at the time of the formation of the second oscillator. Under this interpretation, figure 3 demonstrates how compensating for this *a priori* asymmetric coupling provides control over the state of synchronization of the two oscillators.

With the insights gained by the qualitative discussion above, we model this system with an asymmetric 'integrate and fire' [17] model, which accounts for many of the features encountered

in the experiments. In our model, two oscillators (OL and OR corresponding to the left and right oscillators of figure 2, and the blue and red signals of figure 3) accumulate phases $\phi_L = w_L t$ and $\phi_R = w_R t$ over time (t), where w_L, w_R are the oscillators' frequencies, and generally $w_L \neq w_R$. Whenever ϕ_L (or ϕ_R) accumulates a multiple of 2π phase, it 'fires'—corresponding to the rapid depletion of heat through an hydrothermal wave that ends an oscillation in our system and to the resetting of ϕ_L (or ϕ_R) to zero. A time delay τ after an oscillator has fired, the phase of the other oscillator is incremented by δ_L (or δ_R), corresponding to firing by OL (or OR), respectively. Here, τ corresponds to the time it takes a wave from OL to reach OR or vice versa. Generally, $\delta_L \neq \delta_R$, accounting for the asymmetry of coupling strengths that is inherent to our system.

In figure 4(a), we present theoretical results that were obtained by simulating the model for the experimental conditions presented in figures 3(i)–(v). In figure 3(i), the left oscillator is excited by the right oscillator. The newly formed left oscillator has a low frequency, and it hardly perturbs the phase of the right oscillator. Consequently, the left oscillator becomes synchronized to the right oscillator. Simulating the model under these asymmetric conditions, $w_L < w_R$; $\delta_R > 0$; $\delta_L = 0$, the model predicts this behavior, as presented in figure 4(a)(i).

In the experiment presented in figure 3(ii), the laser beam was moved upward one step. Consequently, the frequency of the left oscillator increases, and the perturbation it causes to the right oscillator's dynamics grows stronger. The left and right oscillators disturb each other irregularly, lacking synchronization. We simulate this experiment with the model, with $w_L > w_R$; $\delta_R > \delta_L > 0$. In figure 4(a)(ii) shows the results of the simulation: the temporal shape of the oscillations becomes irregular and their spectral intensities broaden, in agreement with the experiment presented in figure 3(ii).

Moving the laser further upward, the left and right oscillators perturb each other equally strongly and synchronize in anti-phase, as presented in figure 3(iii). Accordingly, simulating the model for $w_L > w_R$; $\delta_R = \delta_L$, shows the same behavior. We present this result in figure 4(a)(ii).

The chaotic behavior of a single oscillator is not accounted for in our model. However, moving the laser further upward, in figures 3(iv) and (v) the left oscillator becomes dominant—its frequency increases, and the right oscillator frequency-entrains and synchronizes to the left oscillator. Simulating these conditions with our model for $w_L > w_R$; $\delta_L > \delta_R > 0$, the model predicts the same behavior. This result is presented in figure 4(a)(iv).

Figure 4(b) distinguishes between two types of synchronized states. The figure presents magnifications of the spectral intensity of the oscillations in the cases presented in figure 4(a)(iii) (right panel of figure 4(b)) and figure 4(a)(iv) (left panel of figure 4(b)). In both cases, the oscillators are synchronized. However, in figure 4(a)(iii) (right panel of figure 4(b)), the symmetric coupling between the oscillators gives rise to a joint frequency of the oscillations which is neither w_L nor w_R. In contrast, in figure 4(a)(iv) (or left panel of figure 4(b)) the synchronization is strongly asymmetric—the left oscillator forces the right oscillator to follow it and the joint frequency of oscillations is w_L.

5. Conclusions

In this paper, we have presented new light–fluid phenomena arising from the nonlinear feedback between fluid and light, acting in a system where they constantly change. We presented an arrangement in which light–fluid feedback interaction gives rise to local flow patterns in the fluid, which can be set to be synchronized or uncorrelated, by varying the external control parameters. Often in nature, when several sub-systems synchronize, a new functionality arises—a functionality that is not possible with any one of the individual sub-systems alone. Here, the

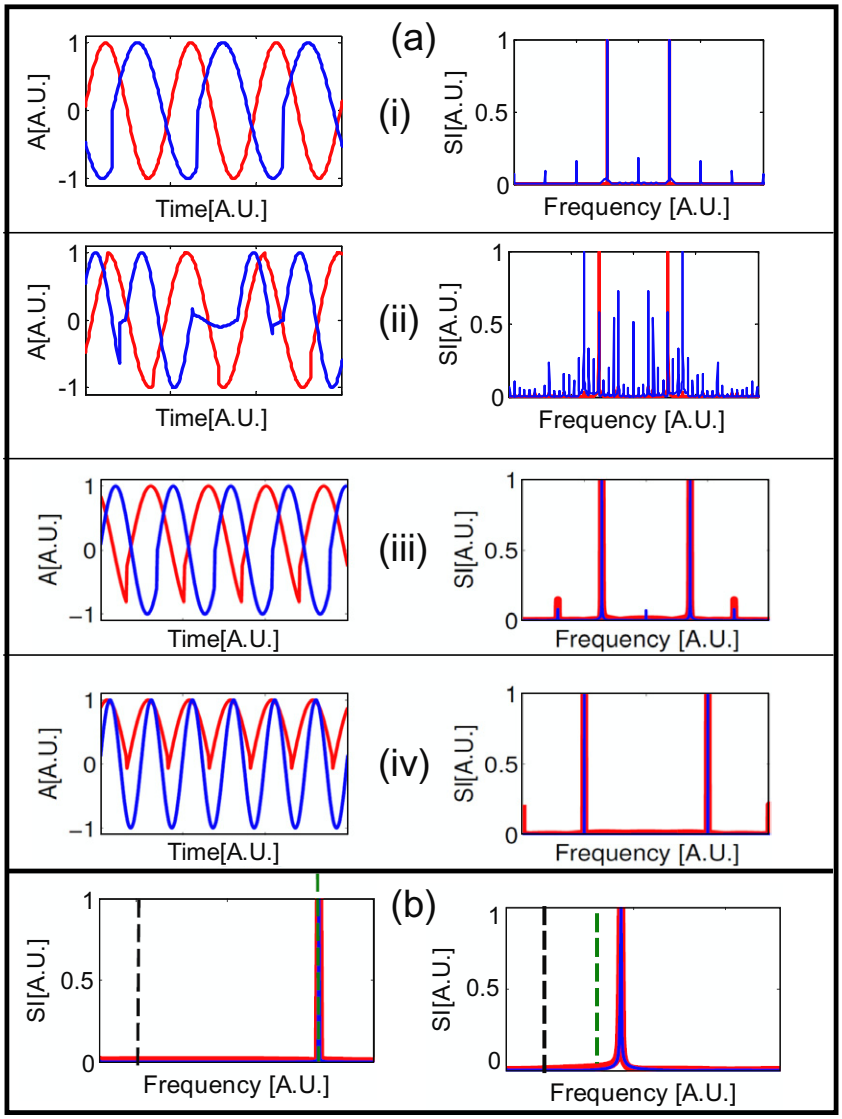

Figure 4. An 'integrate and fire'-type model elucidates the results of figure 3. (a) In each of panels (i)–(iv), the left column is the temporal evolution of the amplitude of oscillation for the left (blue) and right (red) oscillators of figure 3, and the right column presents the corresponding spectral intensities. Panels (i)–(iv) present the modeled oscillations obtained for model parameters corresponding to the experimental situations in figures 3(i), (ii), (iii) and (iv, v), respectively. The results of the model simulations qualitatively reproduce the experimentally observed dynamics presented in figure 3. (b) A magnification of the spectral intensities of panels (iii) and (iv) identifies two distinct states of synchronization. The green and black dashed vertical markers indicate the values of w_{L} and w_{R} for these model simulations, respectively.

new functionality is optical control over the temporal correlation between the oscillations of a flow field in different regions within the fluid. This functionality arises solely by virtue of nonlinear far-from equilibrium dynamics, demonstrating a fundamental concept of nonlinear science in the case of a light–fluid system. We envision that the application of the broader concepts of nonlinear science to light–fluid systems will reveal more useful effects, making possible new functional devices that realize optical control over flow mechanics.

Acknowledgments

We are indebted to Professor Gerard Gouesbet of the University de Rouen, France, Professor Shmuel Fishman of the Technion-Institute of Technology, Israel, and Professor Arkady Pikovsky of the University of Potsdam, Germany, for their enthusiasm, support and helpful suggestions. This work was supported by an Advanced Grant from the European Research Council (ERC) and by the USA–Israel Binational Science Foundation (BSF). E G gratefully acknowledges the support of the Levi Eshkol Fellowship for PhD students.

References

[1] Ladavac K and Grier D G 2004 Microoptomechanical pumps assembled and driven by holographic optical vortex arrays *Opt. Express* **12** 1144–9
[2] Leach J *et al* 2006 An optically driven pump for microfluidics *Lab Chip* **6** 735–9
[3] Liu G L *et al* 2006 Optofluidic control using photothermal nanoparticles *Nat. Mater.* **5** 27–32
[4] Verneuil E *et al* 2009 Laser-induced force on a microfluidic drop: origin and magnitude *Langmuir* **25** 5127–34
[5] Weinert F M and Braun D 2008 Optically driven fluid flow along arbitrary microscale patterns using thermoviscous expansion *J. Appl. Phys.* **104** 104701
[6] Sigel R *et al* 2002 Pattern formation in homogeneous polymer solutions induced by a continuous-wave visible laser *Science* **297** 67–70
[7] Gouesbet G and Lefort E 1988 Dynamical states and bifurcations of a thermal lens using spectral analysis *Phys. Rev.* A **37** 4903–15
[8] Gouesbet G, Rhazi M and Weill M E 1983 New heartbeat phenomenon and the concept of 2-D optical turbulence *Appl. Opt.* **22** 304–9
[9] Gouesbet G, Roze C and Meunier-Guttin-Cluzel S 2000 Instabilities by local heating below an interface *J. Non-Equilib. Thermodyn.* **25** 337–79
[10] Gouesbet G 1990 Simple model for bifurcations ranging up to chaos in thermal lens oscillations and associated phenomena *Phys. Rev.* A **42** 5928–45
[11] Ashkin A 2006 *Optical Trapping and Manipulation of Neutral Particles Using Lasers* (Hackensack, NJ: World Scientific)
[12] Ashkin A, Dziedzic J M and Smith P W 1982 Continuous-wave self-focusing and self-trapping of light in artificial Kerr media *Opt. Lett.* **7** 276–8
[13] Yashin V E *et al* 2005 Formation of soliton-like light beams in an aqueous suspension of polystyrene particles *Opt. Spectrosc.* **98** 466–9
[14] Reece P J, Wright E M and Dholakia K 2007 Experimental observation of modulation instability and optical spatial soliton arrays in soft condensed matter *Phys. Rev. Lett.* **98** 203902
[15] Bernhardt P A 1991 The autonomous chaotic relaxation-oscillator—an electrical analog to the dripping faucet *Physica* D **52** 489–527
[16] Minorsky N 1974 *Nonlinear Oscillations* (Huntington, NY: Krieger)
[17] Pikovsky A, Rosenblum M and Kurths J 2001 *Synchronization: A Universal Concept in Nonlinear Sciences* (*The Cambridge Nonlinear Science Series*) (Cambridge: Cambridge University Press)